Lithium Salt Diffusion in Diblock Copolymer Electrolyte Using Fourier Transform Infrared Spectroscopy

Journal:	*The Journal of Physical Chemistry*
Manuscript ID	jp-2019-11446a.R1
Manuscript Type:	Article
Date Submitted by the Author:	n/a
Complete List of Authors:	Kim, Kyoungmin; FAMU-FSU College of Engineering, Chemical and Biomedical Engineering; Florida State University, Aero-Propulsion, Mechatronics & Energy Center Hallinan, Daniel; Florida A&M University-Florida State University College of Engineering, Chemical and Biomedical Engineering; Florida State University, Aero-Propulsion, Mechatronics & Energy Center

Lithium Salt Diffusion in Diblock Copolymer Electrolyte Using Fourier Transform Infrared Spectroscopy

Kyoungmin Kim,[a,b] *Daniel T. Hallinan Jr.*[a,b,*]

[a] Chemical and Biomedical Engineering Department, Florida Agricultural and Mechanical University–Florida State University College of Engineering, 2525 Pottsdamer Street, Tallahassee, FL 32310, U.S.A.

[b] Aero-Propulsion, Mechatronics & Energy Center, Florida State University, 2003 Levy Avenue, Tallahassee, FL 32310, U.S.A.

ABSTRACT

Diffusion of a lithium salt through a diblock copolymer electrolyte was studied using vibrational spectroscopy. Lithium bis-trifluoromethylsulfonimide (LiTFSI) was dissolved in a lamellar-structured, high-molecular-weight polystyrene–poly(ethylene oxide) diblock copolymer at various concentrations (0 – 4.51 mol_{LiTFSI}/kg_{PEO}). The diffusion coefficient of LiTFSI was determined from time-resolved Fourier Transform infrared spectroscopy attenuated total reflectance (FTIR-ATR) as a function of the salt concentration. By applying the Beer-Lambert law, FTIR-ATR was used to detect concentration changes. Mutual diffusion was driven by putting in contact two polymer electrolyte membranes with different salt concentrations. Thus, mutual diffusion coefficients were obtained without the influence of electric fields or electrode interfaces. The accuracy of the simple experimental approach and straightforward analysis were validated by comparison to diffusion coefficients reported from measurements in electrochemical cells. Both methods yield mutual diffusion coefficients of lithium salt that are only weakly (and non-monotonically) dependent on salt concentration. There is some indication in the spectra that there exist two populations of salt with different dissociation states. This could explain the observed non-monotonic concentration dependence of the mutual diffusion coefficient of the salt. This hypothesis will be examined quantitatively with complementary measurements in future work.

INTRODUCTION

The demand for safe and high-capacity energy storage continues to increase in view of the emergence of applications such as electric vehicles and portable electronic devices. Fundamental challenges for energy storage systems include achieving higher energy density, chemical stability for long lifetime, facile material and device processing, and reasonable cost.[1, 2] In conventional rechargeable (secondary) lithium-ion batteries, lithium ions transport between the anode and the cathode through a liquid electrolyte during charging or discharging. Porous polymer membrane separates the anode and the cathode, and liquid electrolyte fills the pores of the polymer separator to provide ionic transport. Despite the high ionic conductivity, the instability and the flammability of the liquid electrolytes can cause serious safety problems.[3]

Solid polymer electrolytes can replace the liquid electrolytes and polymer separators to enhance safety and chemical stability. An advantage of polymer electrolytes is that they are compatible with lithium metal,[4, 5] which has much higher specific energy than graphite. However, the maximum power (i.e. maximum discharge rate) of a polymer-electrolyte battery is much lower than that of conventional batteries that contain liquid electrolytes. Ionic conductivity of an electrolyte is commonly taken as a direct measure of the maximum charge or discharge rate that can be achieved in a battery. For a binary electrolyte, this is not true even in the dilute limit, where limiting current is a function of salt diffusion coefficient and transference number. It is less clear how a concentrated (non-ideal) electrolyte will perform in a battery, especially if the transport parameters are concentration-dependent. In fact, much less complex systems than polymer electrolytes demonstrate counter-intuitive behavior when analyzed with a complete electrochemical model. For example, supporting electrolyte (which increases conductivity) acts to decrease the limiting current.[6]

The polymer that has been most extensively studied for use as a polymer electrolyte is poly(ethylene oxide) (PEO). It provides ionic conductivity when it dissolves lithium compounds.[7] The low glass transition temperature, T_g, of PEO enables segmental motion of the polymer chain at room temperature, which is the basic transport mechanism of ions in dry polymer electrolytes. On the other hand, the low T_g allows dendrites to grow from the lithium electrode surface. Incorporating PEO into a block copolymer with polystyrene (PS) enhances mechanical strength and suppresses dendrite growth.[8, 9] The ratio of PEO to PS in PS - PEO block copolymer, SEO, dictates morphology, which is important because it impacts both mechanical strength and ionic conductivity.[10]

Lithium bis-trifluoromethylsulfonimide (LiTFSI) is a suitable salt for lithium salt/polymer electrolyte system due to its low dissociation energy and chemical and thermal stability.[11-13] Two strong electron-withdrawing groups stabilize the imide anion and facilitate dissociation.[14] The transport of ions in polymer electrolyte display non-monotonic behavior with salt concentration[15-17] indicating that ion transport is a complex function of various factors, such as polymer dynamics,[18, 19] conformational states of lithium salts,[18] and morphological changes of polymer domains.[19]

Balsara's group has shown that ion transport in polymer electrolytes increases at sufficiently high salt concentration,[19] but their study focused exclusively on low molecular weight SEO, whose microstructure is strongly affected by salt concentration. High molecular weight SEO is of more practical interest, providing the mechanical strength necessary to separate electrodes (and block dendrites) over long-term cycling.[4] Interestingly, high salt concentration has been shown to suppress dendrite formation in liquid electrolytes,[20] perhaps due to double-layer protection.[21] It would be natural to ask if high salt concentration can be combined with polymer mechanical

strength to yield lithium metal batteries with high charge and discharge rates and long lifetimes. A first step is to accurately determine the transport parameters across a broad salt concentration range. The purpose of the present study is to examine the concentration-dependence of the salt diffusion coefficient with time-resolved FTIR-ATR spectroscopy, which yields the mutual diffusion coefficient without the simplifying assumption of thermodynamic ideality.[22] Furthermore, small concentration steps can be used to empirically determine the salt-concentration dependence of the diffusion coefficient. This study is important for improving solid polymer electrolyte battery performance and for demonstrating that time-resolved FTIR-ATR spectroscopy can be used to study diffusion in concentrated, all-solid systems.

Background

Current in a battery can be described by the transport properties of the ions present. To fully represent transport for a binary electrolyte, three independent transport parameters are needed, such as ionic conductivity, κ, salt mutual diffusion coefficient, D, and cation transference number, t_+^0. The maximum current density that can be achieved at steady state is the limiting current density, i_L. Assuming dilute solution in a binary monovalent electrolyte, i_L can be expressed as[23]

$$i_L = \frac{2DFc_{avg}}{(1-t_+^0)L} \quad (1)$$

where F is Faraday's constant, c_{avg} is the average concentration of salt in the electrolyte, and L is the membrane thickness. In concentrated electrolyte, a numerical model would be required to determine the limiting current. However, equation (1) serves to demonstrate the importance of the salt diffusion coefficient in determining the limiting current. Despite its importance, measurement of this diffusion coefficient has been limited by the difficulty of measurement and the complexity of analysis. The diffusion coefficient appearing in equation (1) is a mutual diffusion coefficient of

the salt. In other words, it is measured in the presence of a concentration gradient and quantifies the rate at which the concentration gradient is dissipated by thermally activated random fluctuations of salt molecules (i.e. neutral combinations of ions).

We are aware of three methods that have been used to measure diffusion coefficients in dry polymer electrolytes. Pulsed-field-gradient nuclear magnetic resonance (PFG-NMR) has been used to investigate transference numbers and diffusion coefficients.[15, 16] The diffusion coefficients obtained from PFG-NMR are self-diffusion coefficients of ions (determined in the absence of a concentration gradient). It is possible to calculate a mutual diffusion coefficient of the salt from the self-diffusion coefficients of the ions, if a thermodynamic factor is determined (see Supporting Information). Additional steps are required to determine the thermodynamic factor, which can be quite large in non-ideal, concentrated polymer electrolyte.[15, 24, 25]

Another method is restricted diffusion, which Newman and coworkers have shown to be valid for concentrated systems as well as dilute systems.[26] In the restricted diffusion measurement, the cell potential exponentially decays to the equilibrium potential as the concentration gradient decays to zero due to diffusion. Thus, cell potential is a proxy for concentration gradient, and mutual diffusion coefficient of the salt is being measured. However, concentration-dependence of the salt diffusion coefficient and/or the thermodynamic factor can cause the concentration gradient to be nonlinear. Of course, a calibration can be conducted to relate the cell potential and concentration gradient, but the theoretical relationship between the two is dependent on transference number for which there remains large uncertainty due to complexity of the measurement as well as electrolyte non-ideality.

Our group developed a method to visualize the complete concentration profile in an electrolyte using ^{7}Li magnetic resonance imaging (MRI).[27] By monitoring the concentration profile over time,

the mutual diffusion coefficient of the salt was determined. In this case, MRI intensity is expected to be linearly related to salt concentration. Unlike previous reports that used restricted diffusion, the ^{7}Li MRI study found a strong (exponential) concentration dependence of the mutual diffusion coefficient of LiTFSI in SEO. However, there remains uncertainty regarding the concentration-dependence of the ^{7}Li relaxation times, which affect the measured MRI intensity and could cause it to scale nonlinearly with concentration. It has been reported that the relaxation time can be concentration dependent,[28] and that was not accounted for in our previous MRI study. Thus, another spectroscopic technique is desirable to evaluate the certainty of reported mutual diffusion coefficients of salt in polymer electrolytes.

Fourier transform infrared – attenuated total reflectance (FTIR-ATR) spectroscopy has been used for numerous studies of small molecule diffusion in polymer membranes.[22] It was first validated by Fieldson and Barbari in 1993.[29] Since then it has been used to study diffusion of liquids[30] and vapors[31] with particular emphasis on water sorption in fuel cell membranes[32] and protective coatings.[33] However, to the best of our knowledge it has not been applied to a completely solid system, such as SEO/LiTFSI.

In this report, lithium salt diffusion in diblock copolymer electrolyte is measured with FTIR-ATR spectroscopy. FTIR-ATR spectroscopy has the advantage that it is a measurement without electric current, i.e., concentration gradient is the only driving force for the transport of LiTFSI salt. Another merit of the FTIR-ATR measurement is its relatively simpler and faster analysis as compared to conventional electrochemical methods that have been used in studies of diffusion coefficient of salts in block copolymers. The concentration dependence of the mutual diffusion coefficient of the lithium salt in the block copolymer found in this work agrees with reports using the electrochemical restricted diffusion technique.

EXPERIMENTAL

Materials

A high molecular weight PS-PEO diblock copolymer was synthesized via anionic polymerization.[34] The molecular weights (Mn) of the PS block and the PEO block were 121 kg/mol and 165 kg/mol, respectively. The PEO volume fraction was 0.58 at 90 °C and the polydispersity index of the block copolymer was 1.11. The SEO was freeze dried under vacuum and stored at -20 °C after the synthesis. For polymer electrolyte preparation, the SEO was allowed to warm to room temperature, dried under vacuum at 60 °C, and transferred to an argon-filled glovebox. LiTFSI was mixed with SEO at various concentrations as reported previously.[27] We report the molar ratio of lithium ions to ethylene oxide repeat units in this paper. The molar ratio was denoted as *r,* and the values were between 0 to 0.2. The *r* values of the experiments are shown in Table 1. Thin polymer membranes were cast as described elsewhere.[34] The O_2 and H_2O level in the glovebox were kept under 0.2 ppm during the preparation of the membranes.

Table 1. Molar ratio(*r*) of Li^+ to ethylene oxide of membranes

r	**Test 1**	**Test 2**	**Test 3**	**Test 4**	**Test 5**	**Test 6**	**Test 7**
r_2 (Layer 2)	0.050	0.085	0.105	0.125	0.150	0.170	0.200
r_1(Layer 1)	0.000	0.020	0.050	0.085	0.105	0.125	0.150
$\Delta r = (r_2 - r_1)$	0.050	0.065	0.055	0.040	0.045	0.045	0.050
$r_{\text{avg}} = \left(\frac{r_1 + r_2}{2}\right)$	0.025	0.0525	0.0775	0.105	0.1275	0.1475	0.175
$c_{\text{avg}}(\text{mol}_{\text{LiTFSI}}/\text{kg}_{\text{PEO}})$	0.56	1.18	1.75	2.37	2.88	3.33	3.95

FTIR-ATR

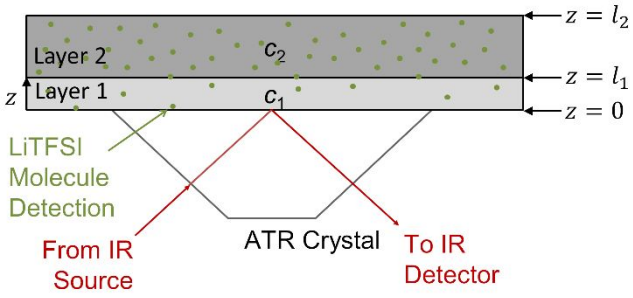

Figure 1. Schematic of two polymer electrolyte membranes on an FTIR-ATR crystal.

Two layers of membranes with different concentrations of lithium salt were prepared. The membrane with the lower concentration (layer 1) was placed on an attenuated total reflectance crystal (Golden Gate™ single reflection diamond ATR, Specac) in a Fourier transform infrared spectrometer (Frontier, Perkin Elmer) acting as a control volume where salt diffuses. A thicker membrane with a higher concentration (layer 2) was placed on a spacer such that it is above layer 1 acting as a source of diffusant with approximately constant concentration. The thicknesses of layer 1 and layer 2, measured before each experiment, were about 100 μm and 400 μm, respectively. The membranes were separated by spacer initially to prevent salt flux during thermal equilibration.

To simplify the analysis, we adopted a differential diffusion method by maintaining a small salt concentration gradient.[35] In this way, the diffusion coefficient can be assumed to be constant over the small concentration range of each experiment, and Fick's second law of diffusion written as

$$\frac{\partial c}{\partial t} = D_{\text{eff}} \frac{\partial^2 c}{\partial z^2} \quad . \qquad (2)$$

D_{eff} is the effective, concentration-averaged diffusion coefficient.

$$D_{\text{eff}} = \frac{\int_{c_1}^{c_2} D(c)dc}{\int_{c_1}^{c_2} dc} \quad (3)$$

where c_1 and c_2 are the concentration of layer 1 and layer 2, respectively. Using differential diffusion with small Δc provides more accurate concentration-averaged diffusion coefficients.[36] In this study, the r differences (Δr) were kept at 0.05 ± 0.015. The concentration of each layer is shown in Table 1 for 7 different tests. At least two measurements were conducted for each test condition. The temperature of the ATR was increased from room temperature to 120 °C within 90 seconds and allowed to equilibrate for 25 minutes. Then layer 2 was pressed into contact with layer 1 (Figure 1). With the two membranes in contact, Li^+ and $TFSI^-$ neutral ion pairs began to transfer from layer 2 to layer 1 via diffusion. Time-resolved infrared spectra were collected by a liquid-nitrogen-cooled mercury-cadmium-telluride (MCT) detector in the wavenumber range of 4000 cm^{-1} to 450 cm^{-1} with 4 scans per spectrum at a resolution of 4 cm^{-1} at intervals of 10 s for 90 minutes.

If there is large thickness difference between l_1 and l_2 ($l_2 - l_1 \gg l_1$, Figure 1), we can assume an infinite diffusant reservoir such that the concentration of layer 2, c_2, is constant during the experiment. The boundary and initial conditions in this case would be

$$c = c_2 \text{ at } z = l_1,\ t > 0 \quad (4)$$

$$\frac{dc}{dz} = 0 \text{ at } z = 0,\ t > 0 \quad (5)$$

$$c = c_1 \text{ at } 0 \le z \le l_1,\ t = 0 \quad (6)$$

An analytical solution to Fick's second law in one-dimension is given: [22, 29, 31, 36, 37]

$$\frac{c - c_1}{c_2 - c_1} = 1 - \frac{4}{\pi} \times \sum_{n=0}^{\infty} \frac{(-1)^n}{2n+1} \exp\left(-Df^2 t\right) \cos\left(fz\right) \quad (7)$$

where

$$f = \frac{(2n+1)\pi}{2l_1} \quad (8)$$

To express the solution in terms of FTIR-ATR absorbance, it must be related to concentration. This can be done by incorporating an expression for the ATR evanescent wave into the Beer-Lambert law with an assumption of weak absorption,

$$A = \int_0^{l_1} \varepsilon c \exp(-2\gamma z) dz \quad (9)$$

where ε is the molar extinction coefficient, and γ is the reciprocal of penetration depth, d_p. Substitution of equation (7) into equation (9) and integration gives

$$\frac{A_t - A_0}{A_{eq} - A_0} = 1 - \frac{8\gamma}{\pi[1 - \exp(-2\gamma l_1)]} \times \sum_{n=0}^{\infty} \frac{1}{2n+1} \left[\frac{\exp(-Df^2 t)[f \exp(-2\gamma l_1) + (-1)^n 2\gamma]}{(2\gamma)^2 + f^2} \right] \quad (10)$$

where A_t is the integrated IR absorbance at time t, A_{eq} is the absorbance at equilibrium, and A_0 is the absorbance at time zero.

RESULTS

FTIR-ATR spectra between 650 cm^{-1} and 1500 cm^{-1} of SEO/LiTFSI electrolyte at 120 ℃ with different *r* values are shown in Figure 2(a). An FTIR-ATR spectrum of pure LiTFSI was measured for comparison and is shown in Figure 2(b). The peak assignments of LiTFSI are shown in Table 2. The asymmetric SO_2 stretch (ν_aSO_2, 1335 cm^{-1})[38-40] and the symmetric SO_2 stretch (ν_sSO_2, 1137 cm^{-1})[38, 39, 41] as well as ν_aSNS (1060 cm^{-1})[39, 40] and ν_aCF_3 (1193 cm^{-1})[38-40] all increase with increasing salt concentration. The ν_sSO_2 (1137 cm^{-1}) and the ν_aSNS (1060 cm^{-1}) overlapped with the COC stretching band (1110 cm^{-1}) of PEO[42, 43] which decreased with increasing salt concentration. The CH_2 twisting (τCH_2, 1250, 1294 cm^{-1})[44] and CH_2 wagging (ωCH_2, 1325, 1350 cm^{-1})[44] on PEO chains overlapped with the ν_aSO_2 band. The ν_aCF_3 band is the most suitable for time-resolved spectroscopic analysis because its change with concentration is most pronounced, and it does not overlap with other peaks.

Representative spectra of the ν_aCF_3 between 1161 cm^{-1} to 1214 cm^{-1} are shown in Figure 3(a). The spectra transition from orange at the beginning of the experiment to blue at final equilibrium, which is at 90 minutes. As shown in Figure 3(a), the ν_aCF_3 peak (1193 cm^{-1}) of $TFSI^-$ increases with increasing time, as the salt diffuses into the region of detection near the crystal surface.

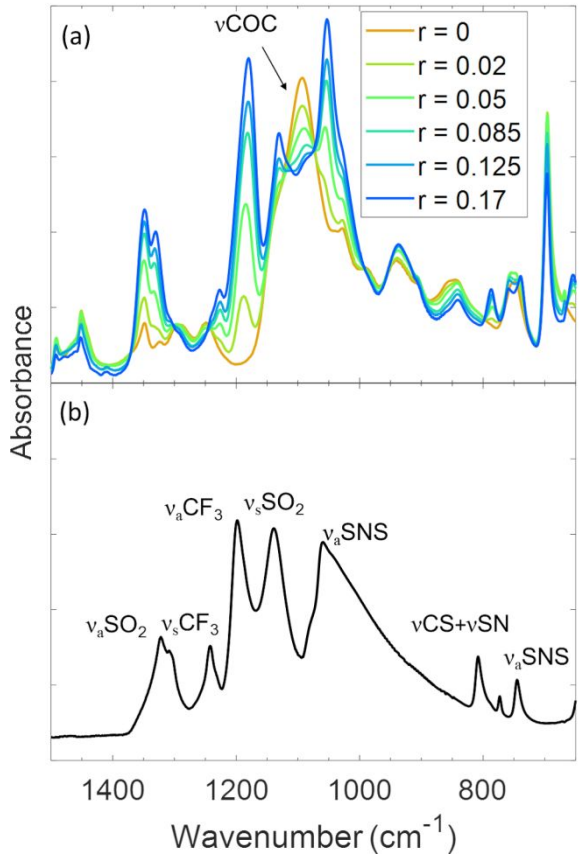

Figure 2. FTIR-ATR spectra of (a) SEO/LiTFSI at various salt concentrations and (b) pure LiTFSI at 120 °C.

Table 2. Infrared band assignment of LiTFSI.

Band Peak (cm^{-1})	Vibration Assignment	Reference
740	ν_sSNS	38-40
790	νCS + νSN	39
1060	ν_aSNS	39, 40
1137	ν_sSO_2	38, 40, 41
1185	ν_aCF_3	38-40
1240	ν_sCF_3	38
1335	ν_aSO_2	38-40

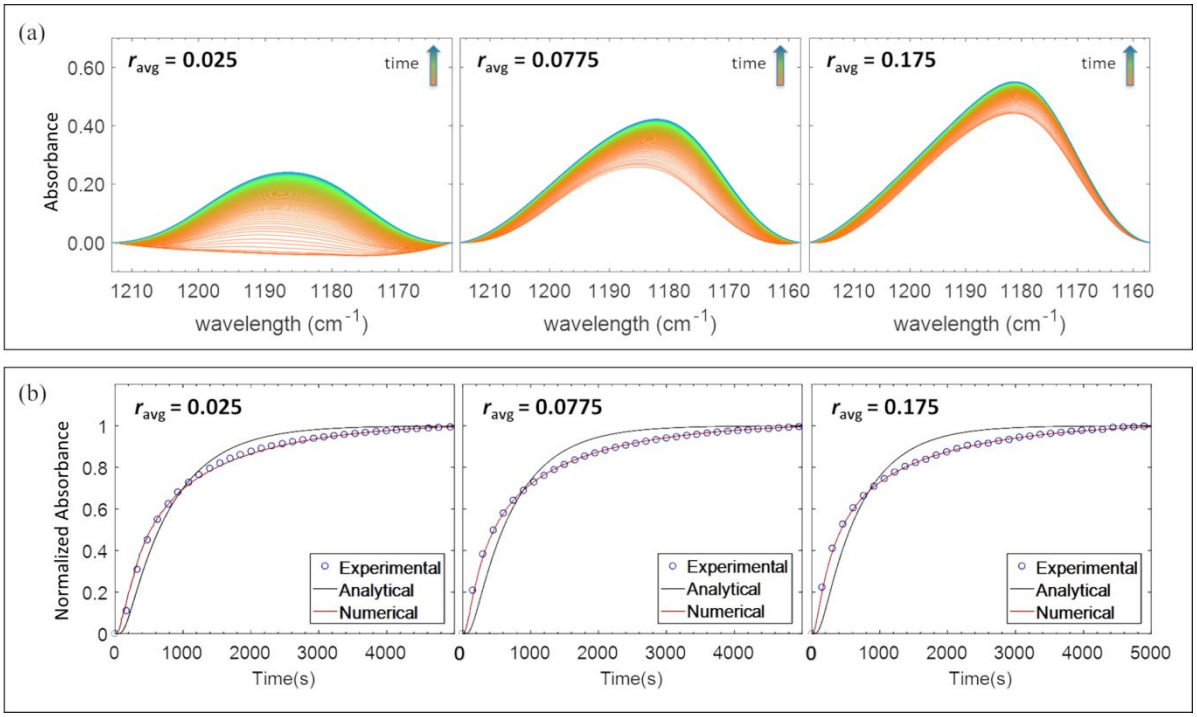

Figure 3. (a) Time-resolved FTIR spectra of asymmetric CF_3 stretching vibration from 0 to 90 minutes at 120 °C. (b) Normalized integration of CF_3 absorbance as a function of time.

Diffusion of the lithium salts was quantitatively analyzed by integrating the area of the spectra of the $\nu_a CF_3$ at each time point and regressing a diffusion model to the normalized integrated absorbance values. The diffusion coefficients were obtained by fitting Equation (10) to the normalized integrated absorbance values.

The results of the modeling are shown in Figure 3(b). The integrated absorbance increased with time. The diffusion coefficients were obtained from the best fit to each data set. The values of the diffusion coefficients are reported in Table S1. The deviation between the experimental data and the model could imply that 1) diffusion is non-Fickian or 2) assumptions or boundary conditions of the analytical model do not properly represent the system. In particular, we assumed that the concentration at the upper boundary of layer 1 is a constant, but the salt concentration is not really

constant during the experiment. To reflect the change of the salt concentration at the interface of the membranes and to allow for a concentration-dependent diffusion coefficient, we conducted numerical analysis of diffusion through both membrane layers, which extended the control volume so that the upper boundary is at l_2 (Figure 1)

$$\frac{\mathrm{d}c}{\mathrm{d}t} = 0 \text{ at } z = 0,\ t > 0 \quad (11)$$

$$\frac{\mathrm{d}c}{\mathrm{d}t} = 0 \text{ at } z = l_2,\ t > 0 \quad (12)$$

and initial conditions

$$c = c_1 \text{ at } 0 \le z \le l_1,\ t = 0 \quad (13)$$

$$c = c_2 \text{ at } l_1 \le z \le l_2,\ t = 0 \quad (14)$$

with the diffusion coefficient allowed to have an exponential dependence on concentration, $D = D_0 \exp(\alpha c)$. The results, however, showed constant diffusion coefficients ($\alpha = 0$) meaning the diffusion coefficient does not significantly change within the concentration range of each test ($\Delta r \le 0.065$).

Salt diffusion was numerically modeled throughout both layers, i.e. with the boundary conditions presented in Equations (11) – (14). Representative regressions of the numerical model are shown in Figure 3(b) and follow the experimental data closely. Although the diffusion coefficients from the numerical analysis were constant within the small concentration increment used in a given test, the salt diffusion coefficient exhibited weak concentration dependence over a wider range of r as shown in Figure 4(a) and reported in Table S1. The average diffusion coefficient for $0 < r_{avg} < 0.15$ from the numerical model is $1.6 \pm 0.3 \times 10^{-7}$ cm^2/s. There is an apparent minimum in D at $r_{avg} = 0.1475$ followed by an increase at $r_{avg} = 0.175$.

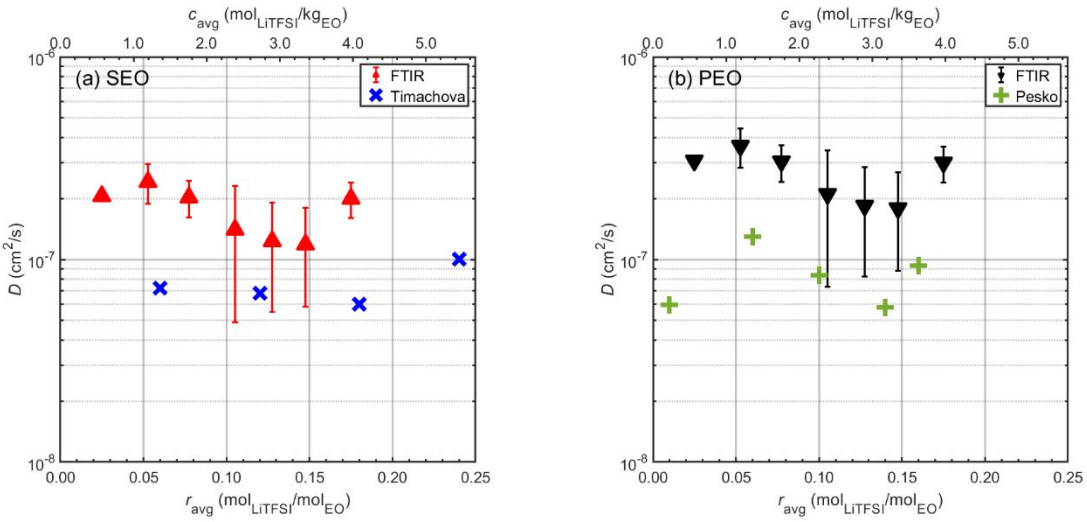

Figure 4. (a) Mutual diffusion coefficients of LiTFSI in SEO membranes from experiment (▲, Mn = 286 kg/mol, 120 °C, FTIR) and reference[16] (×, Timachova et al., Mn = 32 kg/mol, 90 °C, restricted diffusion). (b) Diffusion coefficient of LiTFSI in the conducting phase of SEO membranes (D_c) (▼, 286 kg/mol, 120 °C, FTIR, corrected using morphology factor) and in PEO[15] (+, Pesko et al., Mn = 5 kg/mol, 90 °C, restricted diffusion). The FTIR data are the average of at least two experiments, and the error bars represent one standard deviation. The error bar for the lowest concentration (r_{avg} = 0.025) is not visible because it is smaller than the data point. Error bars are not shown for the references.

DISCUSSION

In Figure 2(b), $\nu_a CF_3$ is at 1200 cm^{-1}, and $\nu_s CF_3$ is at 1243 cm^{-1} for solid LiTFSI. Both symmetric and asymmetric vibration peaks of CF_3 are at lower wavenumber when salt is dissolved in SEO (Figure 2(a)). There is a slight shift of the $\nu_a CF_3$ with increasing salt concentration. This has also been found for LiTFSI dissolved in water. Interestingly, no such shift with salt concentration was found for $\nu_a CF_3$ of LiTFSI in PEO.[41] This might indicate that the presence of PS in SEO has some influence on the chemical environment of the conductive phase. In Figure 2(a), a similar shift is found for νCOC, which could indicate that the shift is due to interaction between the ions and the polymer. Finally, complex changes in shape and magnitude of $\nu_a SNS$ are apparent with increasing concentration. The splitting into two peaks at higher concentrations could be an indication that there are two populations of ions in different dissociation states. This could explain the non-monotonic concentration dependence of the apparent mutual diffusion coefficient of the salt. In future work, we plan to quantitatively analyze these and Raman spectra in an attempt to gain more insight into the physical cause of the non-monotonic concentration dependence of the salt diffusion coefficient.

Diffusion of LiTFSI in lamellar SEO has been reported previously.[27, 45] Timachova et al. reported the mutual diffusion coefficients of LiTFSI in SEO (32 kg/mol, lamellar) in a concentration range from 0.03 to 0.30 of r, at 90 °C by the restricted diffusion method.[16] The values of the diffusion coefficient were between 6.0×10^{-8} and 9.6×10^{-8} cm^2/s, presenting non-monotonic behavior with salt concentration, similar to the results of our study as shown in Figure 4(a). The diffusion coefficient showed a local minimum at $r = 0.18$, while our result has an apparent minimum at $r = 0.1475$. The differences between this study and the reference are the molecular weight and the temperature. The effect of the molecular weight on salt diffusion in SEO was

studied by Mullin et al.[45] The diffusion coefficients of SEOs (r = 0.085) at 90 °C increased with increasing SEO molecular weight and reached a plateau at 30 kg/mol. The plateau value was 8 × 10^{-8} cm^2/s corresponding to the average of Timachova's. Thus, the difference in the absolute values of the diffusion coefficients in Figure 4(a) is most likely due to the two studies being conducted at different temperatures. Diffusion coefficients in condensed phases are known to increase with increasing temperature. The cause of the difference in concentration at which the minimum occurs is unknown but is also potentially due to the temperature difference. This is the subject of further investigation, as temperature can affect ion dissociation state.[46]

A straightforward measurement of diffusion of lithium salts in solid polymer electrolyte was conducted by Chandrashekar et al.[27] The diffusion coefficients of LiTFSI in SEO measured by MRI at 120 °C was found to be concentration-dependent. The concentration dependence was given by an exponential diffusion model, $D = D_0 \exp(\alpha c)$ with α = 21 ± 1 L/mol. The concentration dependence of the mutual salt diffusion coefficient from the MRI study is dramatically different from the weak, non-monotonic concentration dependence seen in the current study. However, the MRI diffusion coefficient calculated at the average concentration of that study (0.8 M) and 120 °C was 2.4 × 10^{-7} cm^2/s, which agrees with our results. As mentioned previously, the exponential dependence could be due to the intensity of MRI being a non-linear function of salt concentration as a result of the ^{7}Li relaxation time being concentration dependent. In the MRI study, the electrolytes were in contact with lithium metal, which can affect the local magnetic field.[47] This could have also contributed to the observed concentration dependence.

The non-monotonic behavior of diffusion coefficient as a function of salt concentration has been observed for homopolymer by Pesko et al.[15] Mutual diffusion coefficients of LiTFSI in 5 kg/mol PEO at 90 ℃ in $0 \leq r \leq 0.16$ were measured using restricted diffusion measurements and are shown

in Figure 4(b).[15] The diffusion coefficients increased until $r = 0.06$ and decreased within $0.06 \leq r \leq 0.14$ and then increased again from the minimum at $r = 0.14$. We note that the diffusion coefficient of the current study cannot be directly compared with those from Pesko et al. due to differences in molecular weight, temperature, and morphology (lamellar block copolymer versus homopolymer).[48] In order to address the morphology difference, it is possible to calculate an effective diffusion coefficient in the conductive phase of SEO (D_c) using the morphology factor, f.[10]

$$D = fD_c \quad (15)$$

D is the measured mutual diffusion coefficient of the salt. The morphology factor is dictated by tortuosity and connectivity of the conducting phase and varies with the block copolymer morphology. Since the block copolymer used in this study has lamellar morphology, f was taken as 2/3, which is the ideal morphology factor for a lamellar-structured block copolymer with randomly oriented grains. Despite the significant difference in molecular weight between the report of Pesko et al. and this work, the trends of the diffusion coefficient as a function of salt concentration agree remarkably well. This calls into question the supposition that the presence of PS in SEO affects the chemical environment of the conductive phase, and motivates a careful look at salt dissociation in both PEO and SEO. Note that the absolute value difference between literature and this work in Figures 4(a) and 4(b) are similar, indicating that the difference is due primarily to the temperature difference. Both literature reports were conducted at 90 °C, whereas this work was conducted at 120 °C.

The reason for the complex behavior of diffusion coefficient has not been explained clearly. It is thought to be related to the salt diffusion mechanism, chain dynamics, and dissociation level of the salt. Studies on the salt dissociation in liquid or polymer electrolytes have reported that the

lithium salts are not fully dissociated at high salt concentration and the associated salts results in ion-pairing effects.[39, 49, 50] In many cases, ion solvation has been implicated to explain concentration dependence of electrolyte transport coefficients.[17, 39, 51-53] Cameron et al. proposed a crosslink model in which anions form crosslinks with cations in neighboring chains at sufficiently high ion concentration. This in turn increases electrolyte viscosity, i.e., decreases diffusivity.[51] The increase of ionic crosslinking with increasing salt concentration has been conventionally accepted, however, quantitative analysis has not been conducted systematically. Hayamizu et al. claimed that mobility decreased due to the larger size of diffusant in concentrated solution where salt dissociation is restricted.[54] The relationship between the degree of dissociation and the transport mechanism is not simple because of the presence of neutral ion pairs and charged single ions. Despite the complexity of possible underlying mechanisms contributing to the non-monotonic concentration dependence of mutual diffusion, mutual diffusion coefficient values (such as those measured with time-resolved FTIR-ATR spectroscopy) are needed to build battery models containing concentrated (non-ideal) electrolytes. They are also the values needed to calculate the limiting current, which dictates the maximum charge/discharge rate of batteries.

FTIR-ATR is a preferable method to qualitatively and quantitatively investigate the dissociation and conformation of species. It provides reliable measurement of mutual diffusion coefficients without additional experimental or mathematical steps. In forthcoming work, FTIR spectroscopy will be complemented with Raman spectroscopy, which is more sensitive to symmetric vibrations than is IR. The two techniques will be used to examine salt dissociation in PEO and SEO polymers with quantitative peak analysis. Correlations between dissociation state populations and transport parameters will be looked for.

CONCLUSIONS

The diffusion of lithium salt in diblock copolymer was studied with time-resolved FTIR-ATR spectroscopy, free from electrodes and electric current. Thus, sample preparation and experimental set-up is simple and analysis is straightforward. The diffusion coefficient of LiTFSI in SEO membranes extracted using a numerical model decreased at low salt concentration then showed an increase at high salt concentration. The weak concentration dependence disagrees with our previous ^{7}Li MRI study but is in agreement with other literature reports. This includes the presence of a shallow local minimum followed by a weak increase of the salt diffusion coefficient at the highest salt concentrations investigated. Further use of spectroscopic measurements such as Raman spectroscopy monitoring the state of salt association are expected to give more fundamental insight into the behavior of the mutual diffusion coefficient of the salt.

ASSOCIATED CONTENT

Theoretical background of the relationship between different types of diffusion coefficients, brief introduction of restricted diffusion technique, and the diffusion coefficients obtained from this study are given in the Supporting Information.

AUTHOR INFORMATION

Corresponding Author

*dhallinan@eng.famu.fsu.edu

Author Contributions

The manuscript was written through contributions of all authors. All authors have given approval to the final version of the manuscript.

ACKNOWLEDGMENT

This work was supported by the National Science Foundation award number 1804871 and the 2017 LG Chem Battery Innovation Contest. The authors would like to acknowledge assistance from the FAMU-FSU College of Engineering Machine Shop.

TOC Graphic

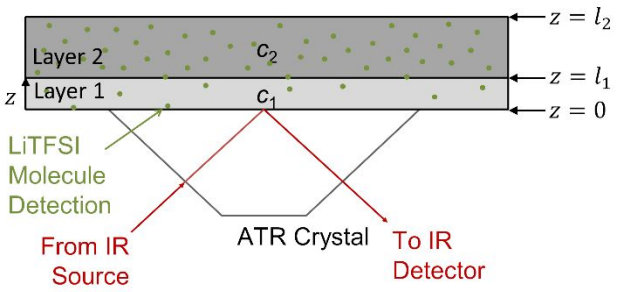

REFERENCES

1. Li, M.; Lu, J.; Chen, Z. W.; Amine, K., 30 Years of Lithium-Ion Batteries. *Adv. Mater.* **2018,** *30* (33), 24.

2. Goodenough, J. B.; Abruna, H.; Buchanan, M. In *Basic Research Needs for Electrical Energy Storage*, Report of the Basic Energy Sciences Workshop for Electrical Energy Storage, 2007.

3. Rosewater, D.; Williams, A., Analyzing System Safety in Lithium-Ion Grid Energy Storage. *Journal of Power Sources* **2015,** *300*, 460-471.

4. Hallinan, D. T.; Mullin, S. A.; Stone, G. M.; Balsara, N. P., Lithium Metal Stability in Batteries with Block Copolymer Electrolytes. *J. Electrochem. Soc.* **2013,** *160* (3), A464-A470.

5. Maslyn, J. A.; Frenck, L.; Loo, W. S.; Parkinson, D. Y.; Balsara, N. P., Extended Cycling through Rigid Block Copolymer Electrolytes Enabled by Reducing Impurities in Lithium Metal Electrodes. *ACS Applied Energy Materials* **2019**.

6. Newman, J., Effect of Ionic Migration on Limiting Currents. *Industrial & Engineering Chemistry Fundamentals* **1966,** *5* (4), 525-529.

7. Wright, P. V., Electrical Conductivity in Ionic Complexes of Poly(ethylene oxide). *British Polymer Journal* **1975,** *7* (5), 319.

8. Monroe, C.; Newman, J., The Impact of Elastic Deformation on Deposition Kinetics at Lithium/Polymer Interfaces. 2005, p A396.

9. Stone, G. M.; Mullin, S. A.; Teran, A. A.; Hallinan, D. T.; Minor, A. M.; Hexemer, A.; Balsara, N. P., Resolution of the Modulus versus Adhesion Dilemma in Solid Polymer Electrolytes for Rechargeable Lithium Metal Batteries. *Journal of the Electrochemical Society* **2012,** *159* (3), A222-A227.

10. Hallinan, D. T.; Villaluenga, I.; Balsara, N. P., Polymer and Composite Electrolytes. *MRS Bulletin* **2018,** *43* (10), 759-767.

11. Seo, D. M.; Borodin, O.; Han, S. D.; Boyle, P. D.; Henderson, W. A., Electrolyte Solvation and Ionic Association II. Acetonitrile-Lithium Salt Mixtures: Highly Dissociated Salts. *Journal of the Electrochemical Society* **2012,** *159* (9), A1489-A1500.

12. Aurbach, D.; Weissman, I.; Zaban, A.; Chusid, O., Correlation between Surface Chemistry, Morphology, Cycling Efficiency and Interfacial Properties of Li Electrodes in Solutions Containing Different Li Salts. *Electrochimica Acta* **1994,** *39* (1), 51-71.

13. Thelen, J. L.; Teran, A. A.; Wang, X.; Garetz, B. A.; Nakamura, I.; Wang, Z. G.; Balsara, N. P., Phase Behavior of a Block Copolymer/Salt Mixture through the Order-to-Disorder Transition. *Macromolecules* **2014,** *47* (8), 2666-2673.

14. Sylla, S.; Sanchez, J. Y.; Armand, M., Electrochemical Study of Linear and Cross-Linked POE-Based Polymer Electrolytes. *Electrochimica Acta* **1992,** *37* (9), 1699-1701.

15. Pesko, D. M.; Timachova, K.; Bhattacharya, R.; Smith, M. C.; Villaluenga, I.; Newman, J.; Balsara, N. P., Negative Transference Numbers in Poly(ethylene oxide)-Based Electrolytes. 2017; Vol. 164, pp E3569-E3575.

16. Timachova, K.; Villaluenga, I.; Cirrincione, L.; Gobet, M.; Bhattacharya, R.; Jiang, X.; Newman, J.; Madsen, L. A.; Greenbaum, S. G.; Balsara, N. P., Anisotropic Ion Diffusion and Electrochemically Driven Transport in Nanostructured Block Copolymer Electrolytes. *Journal of Physical Chemistry B* **2018,** *122* (4), 1537-1544.

17. Ma, Y. P.; Doyle, M.; Fuller, T. F.; Doeff, M. M.; Dejonghe, L. C.; Newman, J., The Measurement of a Complete Set of Transport-Properties for a Concentrated Solid Polymer Electrolyte Solution. *Journal of the Electrochemical Society* **1995,** *142* (6), 1859-1868.

18. Thelen, J. L.; Inceoglu, S.; Venkatesan, N. R.; Mackay, N. G.; Balsara, N. P., Relationship between Ion Dissociation, Melt Morphology, and Electrochemical Performance of Lithium and Magnesium Single-Ion Conducting Block Copolymers. *Macromolecules* **2016,** *49* (23), 9139-9147.

19. Chintapalli, M.; Le, T. N. P.; Venkatesan, N. R.; Mackay, N. G.; Rojas, A. A.; Thelen, J. L.; Chen, X. C.; Devaux, D.; Balsara, N. P., Structure and Ionic Conductivity of Polystyrene-block-poly(ethylene oxide) Electrolytes in the High Salt Concentration Limit. *Macromolecules* **2016,** *49* (5), 1770-1780.

20. Jeong, S.-K.; Seo, H.-Y.; Kim, D.-H.; Han, H.-K.; Kim, J.-G.; Lee, Y. B.; Iriyama, Y.; Abe, T.; Ogumi, Z., Suppression of Dendritic Lithium Formation by Using Concentrated Electrolyte Solutions. *Electrochemistry Communications* **2008,** *10* (4), 635-638.

21. Yang, C.; Chen, J.; Qing, T.; Fan, X.; Sun, W.; von Cresce, A.; Ding, M. S.; Borodin, O.; Vatamanu, J.; Schroeder, M. A.; Eidson, N.; Wang, C.; Xu, K., 4.0 V Aqueous Li-Ion Batteries. *Joule* **2017,** *1* (1), 122-132.

22. Elabd, Y. A.; Baschetti, M. G.; Barbari, T. A., Time-Resolved Fourier Transform Infrared/Attenuated Total Reflection Spectroscopy for the Measurement of Molecular Diffusion in Polymers. *Journal of Polymer Science Part B-Polymer Physics* **2003,** *41* (22), 2794-2807.

23. Newman, J. S.; Thomas-Alyea, K. E., *Electrochemical Systems*. 3rd ed.; J. Wiley: Hoboken, N.J., 2004; p xx, 647 p.

24. Craig, N.; Mullin, S. A.; Pratt, R.; Crane, G. B., Determination of Transference Number and Thermodynamic Factor by use of Anion-Exchange Concentration Cells and Concentration Cells. *J. Electrochem. Soc.* **2019,** *166* (13), A2769-A2775.

25. Stewart, S.; Newman, J., Measuring the Salt Activity Coefficient in Lithium-Battery Electrolytes. *Journal of the Electrochemical Society* **2008,** *155* (6), A458-A463.

26. Newman, J.; Chapman, T. W., Restricted Diffusion in Binary Solutions. *Aiche J.* **1973,** *19* (2), 343-348.

27. Chandrashekar, S.; Oparaji, O.; Yang, G.; Hallinan, D., Communication-Li-7 MRI Unveils Concentration Dependent Diffusion in Polymer Electrolyte Batteries. *Journal of the Electrochemical Society* **2016,** *163* (14), A2988-A2990.

28. Vymazal, J.; Brooks, R. A.; Zak, O.; McRill, C.; Shen, C.; Dichiro, G., T1 and T2 of Ferritin at Different Field Strengths - Effect on MRI. *Magnetic Resonance in Medicine* **1992,** *27* (2), 368-374.

29. Fieldson, G. T.; Barbari, T. A., The Use of FTi.r.-a.t.r. Spectroscopy to Characterize Penetrant Diffusion in Polymers. *Polymer* **1993,** *34* (6), 1146-1153.

30. Elabd, Y. A.; Barbari, T. A., Separating Solvation from Molecular Diffusion in Polymers. *AIChE Journal* **2001,** *47* (6), 1255-1262.

31. Hallinan, D. T., Jr.; De Angelis, M. G.; Baschetti, M. G.; Sarti, G. C.; Elabd, Y. A., Non-Fickian Diffusion of Water in Nafion. *Macromolecules* **2010,** *43* (10), 4667-4678.

32. Kusoglu, A.; Weber, A. Z., New Insights into Perfluorinated Sulfonic-Acid Ionomers. *Chem. Rev.* **2017,** *117* (3), 987-1104.

33. Philippe, L.; Sammon, C.; Lyon, S. B.; Yarwood, J., An FTIR/ATR In Situ Study of Sorption and Transport in Corrosion Protective Organic Coatings - 1. Water Sorption and the Role of Inhibitor Anions. *Progress in Organic Coatings* **2004,** *49* (4), 302-314.

34. Oparaji, O.; Zuo, X.; Hallinan Jr, D. T., Crystallite Dissolution in PEO-Based Polymers Induced by Water Sorption. *Polymer* **2016,** *100*, 206-218.

35. Billovits, G. F.; Durning, C. J., Linear Viscoelastic Diffusion in the Polystyrene/Ethylbenzene System: Differential Sorption Experiments. *Macromolecules* **1993,** *26* (25), 6927-6936.

36. Hallinan, D. T.; Elabd, Y. A., Diffusion of Water in Nafion Using Time-Resolved Fourier Transform Infrared-Attenuated Total Reflectance Spectroscopy. *Journal of Physical Chemistry B* **2009,** *113* (13), 4257-4266.

37. Hallinan, D. T.; Elabd, Y. A., Diffusion and Sorption of Methanol and Water in Naflon using Time-Resolved Fourier Transform Infrared-Attenuated Total Reflectance Spectroscopy. *Journal of Physical Chemistry B* **2007,** *111* (46), 13221-13230.

38. Vélez, J. F.; Aparicio, M.; Mosa, J., Effect of Lithium Salt in Nanostructured Silica–Polyethylene Glycol Solid Electrolytes for Li-Ion Battery Applications. *The Journal of Physical Chemistry C* **2016,** *120* (40), 22852-22864.

39. Pennarun, P. Y.; Jannasch, P., Influence of the Alkali Metal Salt on the Properties of Solid Electrolytes Derived from a Lewis Acidic Polyether. *Solid State Ionics* **2005,** *176* (23-24), 1849-1859.

40. Kam, W.; Liew, C.-W.; Lim, J.; Ramesh, S., Electrical, Structural, and Thermal Studies of Antimony Trioxide-Doped Poly(acrylic acid)-Based Composite Polymer Electrolytes. *Ionics* **2014,** *20* (5), 665-674.

41. Rey, I.; Lassegues, J.; Grondin, J.; Servant, L., Infrared and Raman Study of the PEO-LiTFSI Polymer Electrolyte. *Electrochimica Acta* **1998,** *43* (10-11), 1505-1510.

42. Davison, W. H. T., Infrared Spectra and Crystallinity. Part III. Poly(ethylene glycol). *Journal of the Chemical Society* **1955**, 3270-&.

43. Chu, P. P.; Reddy, M. J.; Tsai, J., Structural and Transport Characteristics of Polyethylene Oxide/Phenolic Resin Blend Solid Polymer Electrolytes. *Journal of Polymer Science Part B-Polymer Physics* **2004,** *42* (21), 3866-3875.

44. Dissanayake, M.; Frech, R., Infrared Spectroscopic Study of the Phases and Phase-Transitions in Poly(ethylene oxide) and Poly(ethylene oxide)-Lithium Trifluoromethanesulfonate Complexes. *Macromolecules* **1995,** *28* (15), 5312-5319.

45. Mullin, S. A.; Stone, G. M.; Panday, A.; Balsara, N. P., Salt Diffusion Coefficients in Block Copolymer Electrolytes. *Journal of the Electrochemical Society* **2011,** *158* (6), A619-A627.

46. Oparaji, O. D. The Influence of Molecular Transport on the Structure-Property Relationships of Amphiphilic Block Copolymer Membranes. Florida State University, 2017.

47. Galluzzo, M. D.; Halat, D. M.; Loo, W. S.; Mullin, S. A.; Reimer, J. A.; Balsara, N. P., Dissolution of Lithium Metal in Poly(ethylene oxide). *ACS Energy Lett.* **2019,** *4* (4), 903-907.

48. Shi, J.; Vincent, C. A., The Effect of Molecular-Weight on Cation Mobility in Polymer Electrolytes. *Solid State Ionics* **1993,** *60* (1-3), 11-17.

49. Jeschke, S.; Wiemhofer, H. D., FTIR and DFT Studies of LiTFSI Solvation in 3-Methyl-2-Oxazolidinone. *Spectrochimica Acta Part a-Molecular and Biomolecular Spectroscopy* **2016,** *157*, 220-226.

50. Wen, S. J.; Richardson, T. J.; Ghantous, D. I.; Striebel, K. A.; Ross, P. N.; Cairns, E. J., FTIR Characterization of PEO+LiN(CF3SO2)(2) Electrolytes. *Journal of Electroanalytical Chemistry* **1996,** *408* (1-2), 113-118.

51. Cameron, G. G.; Ingram, M. D.; Sorrie, G. A., The Mechanism of Conductivity of Liquid Polymer Electrolytes. *Journal of the Chemical Society-Faraday Transactions I* **1987,** *83*, 3345-3353.

52. Metwalli, E.; Rasool, M.; Brunner, S.; Muller-Buschbaum, P., Lithium-Salt-Containing High-Molecular-Weight Polystyrene-block-Polyethylene Oxide Block Copolymer Films. *Chemphyschem* **2015,** *16* (13), 2882-2889.

53. Zugmann, S.; Fleischmann, M.; Amereller, M.; Gschwind, R. M.; Wiemhofer, H. D.; Gores, H. J., Measurement of Transference Numbers for Lithium Ion Electrolytes via Four Different Methods, a Comparative Study. *Electrochimica Acta* **2011,** *56* (11), 3926-3933.

54. Hayamizu, K.; Matsuo, A.; Arai, J., A Divalent Lithium Salt Li2B12F12 Dissolved in Propylene Carbonate Studied by NMR Methods. *Journal of the Electrochemical Society* **2009,** *156* (9).

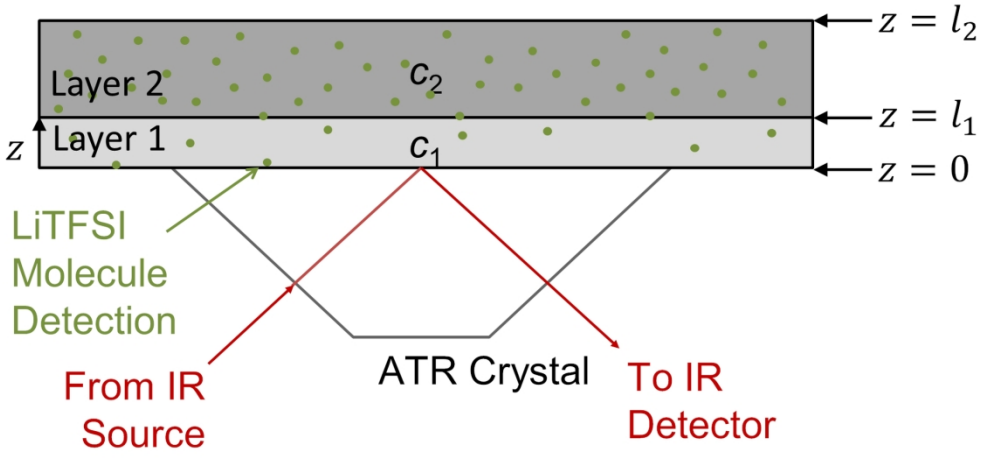

Figure 1. Schematic of two polymer electrolyte membranes on an FTIR-ATR crystal.

84x41mm (600 x 600 DPI)

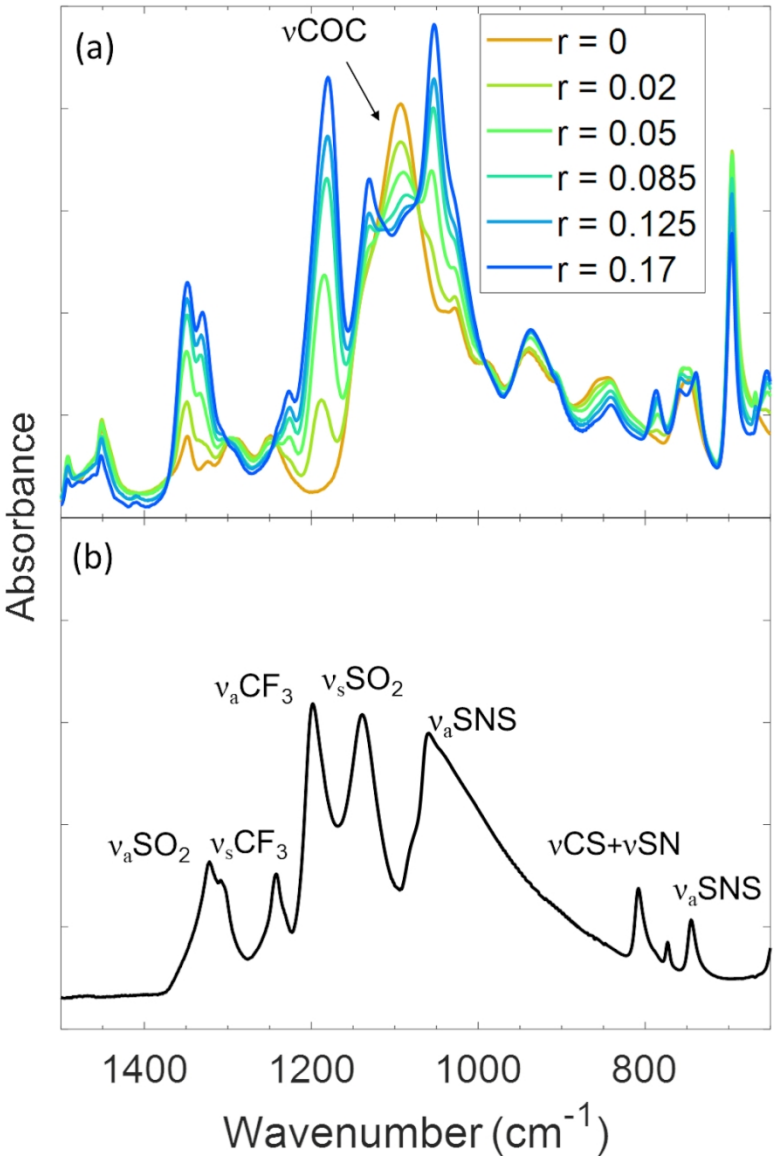

Figure 2. FTIR-ATR spectra of (a) SEO/LiTFSI at various salt concentrations and (b) pure LiTFSI at 120 °C

84x117mm (340 x 340 DPI)

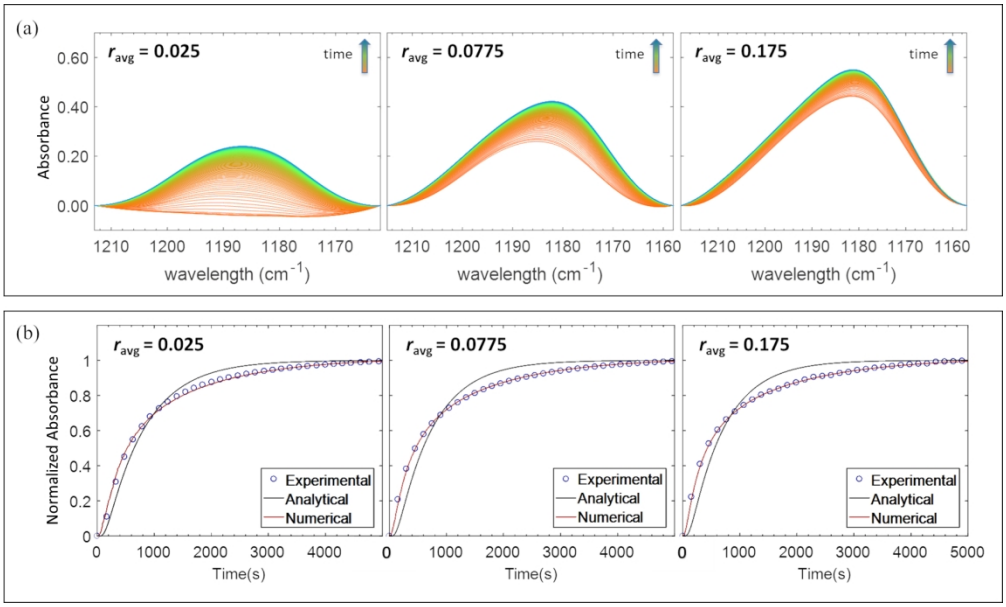

Figure 3. (a) Time-resolved FTIR spectra of asymmetric CF3 stretching vibration from 0 to 90 minutes at 120 °C. (b) Normalized integration of CF3 absorbance as a function of time.

156x93mm (300 x 300 DPI)

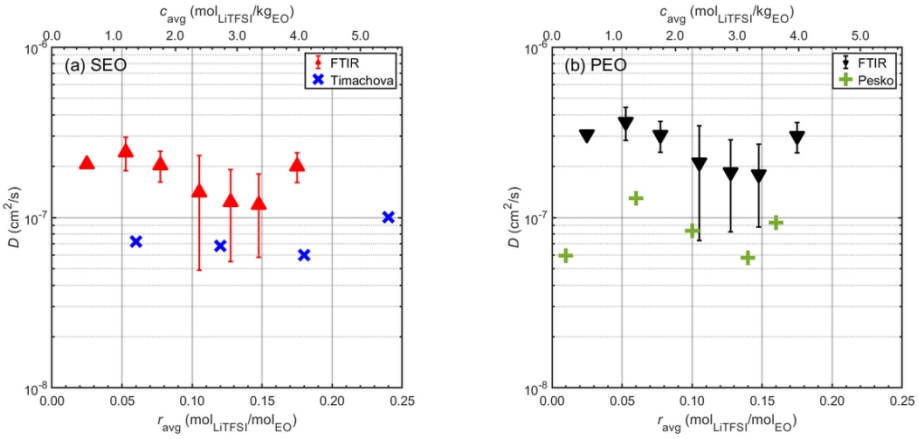

Caption : Figure 4. (a) Mutual diffusion coefficients of LiTFSI in SEO membranes from experiment (▲, Mn = 286 kg/mol, 120 °C, FTIR) and reference16 (×, Timachova et al., Mn = 32 kg/mol, 90 °C, restricted diffusion). (b) Diffusion coefficient of LiTFSI in the conducting phase of SEO membranes (Dc) (▼, 286 kg/mol, 120 °C, FTIR, corrected using morphology factor) and in PEO15 (+, Pesko et al., Mn = 5 kg/mol, 90 °C, restricted diffusion). The FTIR data are the average of at least two experiments, and the error bars represent one standard deviation. The error bar for the lowest concentration (ravg = 0.025) is not visible because it is smaller than the data point. Error bars are not shown for the references.

105x51mm (300 x 300 DPI)